Bionatura Journal
Ibero-American Journal of Biotechnology and Life Sciences

Article

Silver Nanoparticles Loaded with Bark Extract of *Sterculia foetida*: Their Green Synthesis, Characterization, and Anti-bacterial Activity Evaluation

Koushik Jana[1*], *Somnath Ghosh*[2], *Abhijit Ghosh*[3], *Pijus Parua*[4], *Surashree Samanta*[5], *Sonjit Das*[6], *Biplab Debnath*[7]

[1]*Department of Phacognosy, Bharat Technology, Jadurberia, Uluberia, Howrah, West Bengal, 711316, India. Email- koushikjana880@gmail.com,*

[2]*Department of Pharmaceutical Technology, Bharat Technology, Jadurberia, Uluberia, Howrah, West Bengal, 711316, India. Email- gsomnath9734@gmail.com,*

[3]*Department of Pharmacognosy, Bharat Technology, Jadurberia, Uluberia, Howrah, West Bengal, 711316, India. Email- ghosh.abhjit99@gmail.com,*

[4]*Department of Pharmaceutical Technology, Bharat Technology, Jadurberia, Uluberia, Howrah, West Bengal, 711316, India. Email- pijusparua310@gmail.com,*

[5]*Department of Pharmacognosy, Bharat Technology, Jadurberia, Uluberia, Howrah, West Bengal, 711316, India. Email- surashreesamanta2001@gmail.com ,*

[6]*Department of Pharmacy, Regional Institute of Paramedical and Nursing Science, Zemabawk, Aizawl, Mizoram,796017, India. Email- dsonjit@gmail.com,*

[7]*Department of Pharmaceutical Chemistry, Bharat Technology, Uluberia, Howrah, West Bengal, 711316, India. Email- biplab.d86@gmail.com,*

**Correspondance. koushikjana880@gmail.com Mobile number: 7001088536*

ABSTRACT

Sterculia foetida is a subject of interest in many scientific fields as researchers look for novel treatments because of its varied medicinal qualities and chemical richness. Terpenoids are aromatic and aliphatic chemicals with anti-bacterial properties and can prevent free radical damage. They are present in *S. foetida* extract. Moreover, it possesses immunomodulatory, hepatoprotective, antiviral, antioxidant, anti-inflammatory, and antifungal properties. This work aims to green synthesize, characterize, and evaluate the anti-bacterial activity of *Sterculia foetida* bark extract-loaded silver nanoparticles. Chemicals like Methanol, Petroleum Ether, and water have been used to extract the phytoconstituents from the plant bark. $AgNO_3$ and Silver have been used to synthesize the nanoparticles. Instruments like ATR-IR Spectrophotometer, UV-spectrophotometer, DLS, and SEM instruments have been used to characterize the nanoparticles. Bacterial strains like *Staphylococcus aureus* (ATCC-6538), *Escherichia coli* (ATCC 25922), saline water, AMX^{30}, swab stick, inoculation loop, susceptibility scale have been used for studying the anti-bacterial activity. DLS and zeta potential analysis demonstrated the creation of stable nanoparticles with a particle size of 79 nm. The anti-bacterial activity of AgNPs with the methanolic bark extract showed significant anti-bacterial activity compared to the standard marketed drug AMX^{30}. The highest zone of inhibition was observed against gram-positive bacteria *S.aureus* (1.68 cm) and gram-negative bacteria *E.coli* (1.74 cm), respectively, at 500 µg/ml

concentration. The study concludes that greenly synthesized *S. foetida* bark extract containing nanoparticles is a potential anti-bacterial agent, especially against gram-negative bacteria. Further, *in vivo* studies are needed to establish its potential.

Keywords: Sterculia foetida, Green synthesis, Silver Nanoparticles (AgNPs), ATR-IR, DLS, SEM, Zeta-potential, Anti-bacterial.

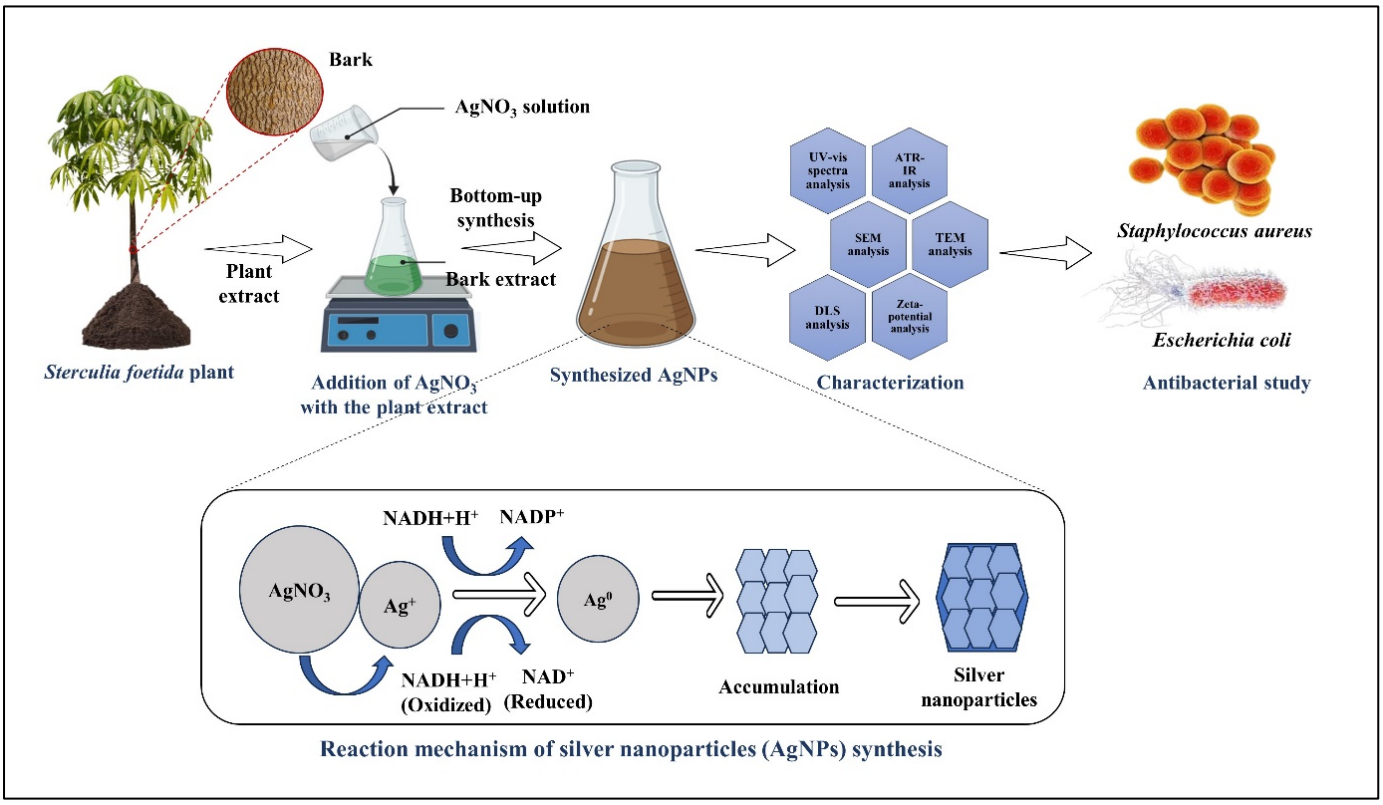

GRAPHICAL ABSTRACT: The collected bark of *S. foetida* was processed to extract phytochemicals. $AgNO_3$ solution was then added to the bark extract, and through oxidation and reduction reactions, silver nanoparticles were formed under constant temperature, pH, and agitation. These nanoparticles were characterized using DLS, UV-visible spectroscopy, ATR-IR, Zeta potential, and SEM analysis. Finally, the anti-bacterial activity was evaluated against *S. aureus* and *E. coli.*

INTRODUCTION

Nanotechnology has gradually permeated various global industries. This swift technological evolution is particularly evident in developed regions, where nanoscale markets have rapidly expanded over the past decade[1]. Nanotechnology bridges classical and quantum mechanics within a mesoscopic system, facilitating the production of natural nanoformulations. These nanoformulations are utilized in diverse fields such as agriculture, nanomedicine, and medical diagnostics and treatment tools[2]. In recent years, significant attention has been paid to using nanotechnology in pharmacy, medicine, and plant sciences, both within living organisms and inorganic systems.

Nanoscale particles exhibit enhanced properties due to atomic interactions at their surfaces, which differ from the coordination seen in bulk materials[3]. These nanoparticles (NPs) can be composed of either metals or nonmetals, depending on their fundamental structure. Metallic NPs typically include gold, Silver, copper, magnetic materials such as cobalt and nickel, and semiconductors. Significant research has focused on metallic NPs due to their unique electrical, optical, and catalytic characteristics[4]. Silver nanoparticles (AgNPs) are recognized as highly effective metallic NPs. They demonstrate catalytic solid and conductive properties, significantly contributing to photochemistry, biomedicine, and agriculture. AgNPs are notable for their

exceptional antimicrobial, antiviral, and biocompatible characteristics and promising advancements in biomedical applications such as microbial resistance, sunscreen formulations, and photochemical processes[5]. Physical, chemical, and green synthesis are standard methods for synthesizing AgNPs. The limitations of physical and chemical processes in producing AgNPs are well-documented, primarily due to associated risks such as cytotoxicity, carcinogenicity, genotoxicity, and overall toxicity. In response to these concerns, there is growing interest in green synthesis techniques utilizing plants, bacteria, yeast, actinomycetes, algae, viruses, and fungi. These methods have garnered attention for their non-toxic nature, safety for humans, simplicity, eco-friendliness, and cost-effectiveness, offering promising alternatives to traditional synthesis approaches[6]. AgNPs can be synthesized using two main approaches: top-down and bottom-up. Using methods like laser ablation and sputtering, the top-down approach reduces bulk materials into nanoparticles. In contrast, the bottom-up approach entails constructing NPs from smaller entities using techniques such as chemical and biological processes[7]. Throughout history, the bactericidal properties of silver ions (Ag+) have been recognized. This understanding dates back to ancient times and is evident in solutions such as "Holy water," which has been used since the first millennium to prevent microbial infections. The presence of silver ions and AgNPs has been confirmed through research on such solutions. These compounds demonstrate various antimicrobial activities, such as bacteriostatic, antiviral, antifungal, and bactericidal actions against different pathogenic bacteria, yeast fungi, and viruses[8].

Interestingly, their inhibitory effects may sometimes surpass those of conventional antibiotics like penicillin and bleomycin, particularly considering the growing resistance of many microorganism strains to antibiotics[9]. AgNPs function by continuously releasing Ag ions, which serve as the primary mechanism for microbe eradication. These ions have a great affinity and electrostatic attraction to sulfur proteins, which allows them to stick to the cytoplasmic membrane and cell wall[10]. The disruption of the bacterial envelope results from this adhesion's membrane permeability enhancement. When cells take up free silver ions, their respiratory enzymes become inactive, which leads to the creation of reactive oxygen species and inhibits the synthesis of adenosine triphosphate. Reactive oxygen species are crucial in rupturing cell membranes and modifying DNA[11]. The interaction between silver ions and sulfur and phosphorus within DNA might hinder DNA replication and cell reproduction, potentially resulting in microbiological termination since these elements are essential components of DNA[12]. Moreover, ribosomes in the cytoplasm can be denatured by silver ions, which prevents the synthesis of new proteins (Figure 1).

AgNPs have historically been synthesized using natural substances such as *Camellia sinensis*, *Sesbania drummondii*, *Sterculia foetida, Aloe vera*, *Azadirachta indica,* various leaf extracts, lemongrass leaves extract, natural rubber, starch, and similar resources. Among these *Stercculia foetida* (Figure 2), commonly known as Wild Almond, Java Olive, Kutiraippitukkan (Tamil), Jangli Badam (Hindi), Bhatala Penari (Kannada), Kuvem ruk (Konkani), Pinar (Malayalam), Adavibadamu (Telugu) and Putidaru (Sanskrit) and it belongs to the Malvaceae family. The anti-bacterial properties of this plant make it a well-known medicine[13–17]. *S. foetida* is a topical plant Indigenous to East India, Sri Lanka, Myanmar, and Thailand[18]. Ethanolic leaves extracts of *S. foetida* have been reported to contain five to eight compounds like apigenin-6, 8-di-C-beta-D-glucoside, 5,7,8-tetrahydroxy-4'-methoxyflavone, puerarin, 5,7,8-tetrahydroxy-4'-methoxyflavone-8-O beta-D-glucoside, 5,7,8-tetrahydroxy-3',4' dimethoxyflavone, which shows antimicrobial activity[19–21]. Seeds, roots, and flowers contain sterculic acid, malvalic acids, leucoanthocyanidin-3-alpha- L-rhamnopyranoside, quercetin, rhamnoside, and fatty acids, which show anti-rheumatic and anti-inflammatory activity[22,23]. The GC-MS analysis of the methanolic bark extract identified 34 phytoconstituents. Among these, the most abundant were Lupeol (63.81%), Lup-20(29)-en-3-one (5.54%), n-Hexadecenoic acid (5.73%), Stigmast-5-en-3-ol oleate (1.94%), Vanillic acid (1.22%), Nonacosane (0.99%), 9-Octadecenoic acid (Z)- methyl ester (0.46%), Tetracosane (0.71%), Tris(2,4-di-tert-butylphenyl) phosphate (0.65%), and Calcifediol (0.62%). These compounds are noted for their anti-bacterial, antifungal, antioxidant, antimicrobial, anti-inflammatory, and wound-healing properties, as detailed in Table 1[24]. Historically the use of 3-d-glucose, biopolymer-based green synthesis of NPs[25] has enhanced the area of interest in finding the phytochemical extracts loaded with silver NPs. Previously, the synthesis of AgNPs from plant extracts like *Aloe vera*, *Carica papaya*, *Azadirachta indica*, *Emblica officinalis*, *Jatropha curcas, Cuminum cyminum, Stigmaphyllon littorale, Boswellia serrata*, *Securinega leucopyrus,* etc has also been reported. Green synthesis of AgNPs was also reported using soluble

starch[26]. There have also been reports on the green synthesis, characterization, and antibacterial activity of AgNPs made with an aqueous extract of young leaves of *S. foetida*[27]. Notably, there is a dearth of significant research on the methanolic extract of the bark, suggesting a need for the development of a new antimicrobial agent from this source. AgNPs have emerged as a promising alternative to combat antimicrobial-resistant bacteria and fungi. Plant-based AgNPs, with their broad spectrum of antimicrobial activity, are particularly preferred over chemically synthesized counterparts due to the surface chemical functionalization of bioactive compounds, enhancing their physio-chemical properties for interaction with microbes through multiple pathways, thereby achieving higher antimicrobial efficiency.

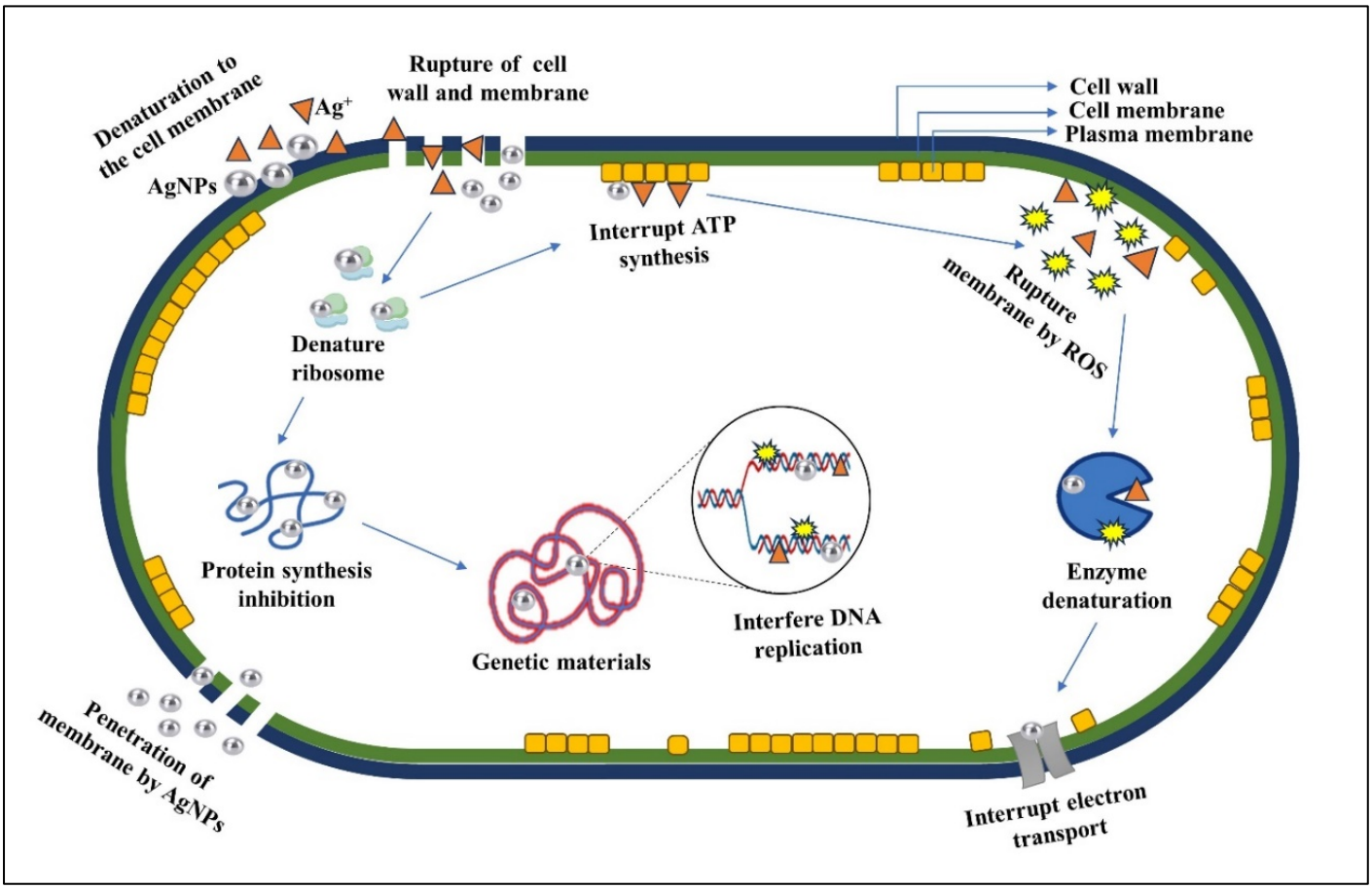

Figure 1. Schematic pathway of proposed approaches of silver nanoparticles against bacteria.

Sl. no	Name of compounds	Chemical formula	Molecular weight	Class of compound	Active on which type of bacteria	Structure of compounds	Ref
1	Lupeol	$C_{30}H_{50}O$	426	Triterpenoids	Gram-negative and gram-positive	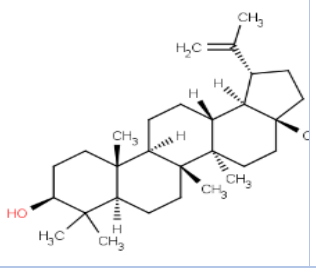	28,29

2	Lup-20(29)-en-3-one	$C_{30}H_{48}O$	424	Triterpenoids	Gram-negative and gram-positive	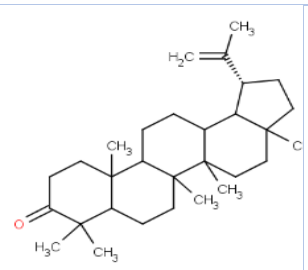	30,31
3	n-Hexadecenoic acid	$C_{16}H_{32}O_2$	256	Fatty acid	Gram-negative and gram-positive	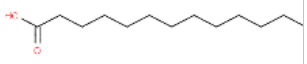	32,33
4	Stigmast-5-en-3-ol, oleate	$C_{47}H_{82}O_2$	678	Beta-sitosterol	Gram-negative and gram-positive	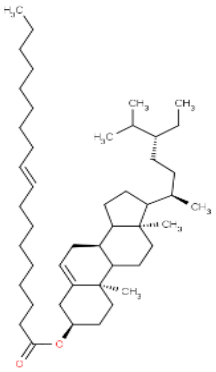	34,35
5	Vanillic acid	$C_8H_8O_4$	168	Phenolic compound	Gram-negative	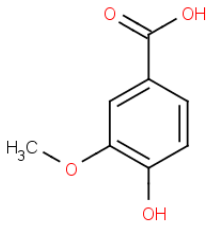	36
6	Nonacosane	$C_{29}H_{60}$	408	Alkane	Gram-positive		37,38
7	9-Octadecenoic acid (Z)-, methyl ester	$C_{19}H_{36}O_2$	296	Ester	Gram-negative and gram-positive	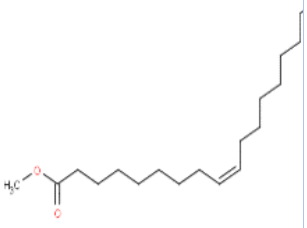	39,40
8	Tetracosane	$C_{24}H_{50}$	338	Alkane	Gram-negative and gram-positive	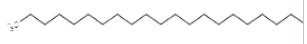	20,41

9	Tris(2,4-di-tert-butylphenyl) phosphate	$C_{42}H_{63}O_4P$	662	Aryl phosphate	Gram-positive	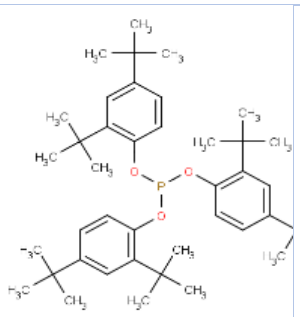	21
10	Calcifediol	$C_{27}H_{44}O_2$	400	Vitamin	-	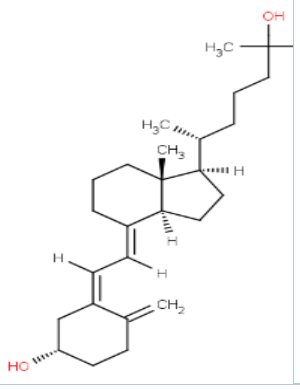	30,38

Table 1. Review of compounds of the bark extract of *S. foetida* plant showing antibacterial activity.

Figure 2. Image of plant *Sterculia foetida*

MATERIAL AND METHODS

Collection, authentication, and identification of plant

S. foetida was collected from rural Uluberia in Howrah, West Bengal, India, and identified by Dr. K. Karthigeyan, SScientist','' under the voucher number CNH/Tech.II/2022/126 at the Botanical Survey of India,

Central National Herbarium, Howrah, 711103. The Department of Pharmacognosy at Bharat Technology, Uluberia, Howrah, West Bengal 711316, also holds the herbarium of this plant species.

Collection of chemicals and instruments

Chemicals like Petroleum Ether, Ethyl acetate, Methanol, Distilled water, $AgNO_3$, Quercetin, Gallic acid, and Folin-Ciocalteu reagent have been collected from the laboratory of Bharat Technology.

Instruments like Analytical Balance, ATR-IR Spectrophotometer, UV-spectrophotometer, DLS instrument, and SEM instrument have also been from the central instrument laboratory of Bharat Technology.

The bacterial strains like *Escherichia coli* (ATCC 25922) and *Staphylococcus aureus* (ATCC-6538). Media plate, Saline water, AMX^{30}, Swab stick, Inoculation loop, and Susceptibility scale have also been collected from Bharat Technology for antimicrobial activity study.

Preparation of Extracts:

The bark of *S. foetida* was collected from uncultivated areas, shade-dried, and ground into a powder using a mixer grinder. Approximately 1.5 kg of this bark powder was placed in a beaker. To remove chlorophyll and lipids, petroleum ether was used, and the extract was then subjected to successive solvent extraction in order of polarity using petroleum ether, ethyl acetate, methanol, and distilled water through a Soxhlet apparatus. The extracts were filtered with Whatman filter paper (11µm), and the crude extract was dried using a rotary vacuum evaporator. The percentage yields of the extracts were then measured and stored in a desiccator for further analysis.

Synthesis of silver nanoparticles

Silver nanoparticles of *S. foetida* were synthesized using three different concentrations of $AgNO_3$ solution: 0.025 M, 0.05 M, and 0.1 M. For each concentration, 20 ml of the bark extract (1.7 g/100 ml) was mixed with 80 ml of the respective aqueous $AgNO_3$ solution in a 1:4 ratio. The methanolic extract (10 ml) was gradually added to the precursor solution at intervals of five minutes until noticeable color changes were seen. A magnetic stirrer continuously heated the final mixture between 65 and 70^0C for 2.5 hours. The mixture was observed at various intervals to track the entire silver nanoparticle (AgNP) formation process. A color shift to dark brown in the solution signified the creation of AgNPs. The impact of pH changes on the synthesis of AgNPs was examined, with adjustments made using 1N HCl or NaOH and measurements taken with a Conductronic PH140 pH meter. The solutions were centrifuged for five minutes at 5000 rpm after incubation. Following centrifugation, the supernatant was disposed of, and the AgNPs underwent a thorough washing process before being dried for a few hours at 100°C in an oven.

Characterization of silver nanoparticles

Visual Observation-

The naked eye can observe the color of the solution under the formation of the nanoparticles. Exposure to the proper solution formulation led to rapidly reducing the $AgNO_3$ mixture to extract the S. foetida during the exercise.

UV-Visible spectra analysis-

AgNPs' optical characteristics were ascertained using a Shimadzu UV model 1780 UV-visible spectrophotometer. After adding $AgNO_3$ to the plant extract, spectra were obtained between 350 and 500 nm at various intervals for up to 24 hours. Following the addition of $AgNO_3$ for 24 hours, the spectra were obtained.

Attenuated Total Reflectance Infra-Red Spectroscopy (ATR-IR) Analysis

An ATR-IR spectrometer (Shimadzu IR Spirit T ATR) was used to analyze the chemical makeup of the produced silver nanoparticles. After the AgNPs were dried at 75^0C, the dried powder's properties were measured between 4000 and 400 cm^{-1}.

DLS & Zeta-Potential analysis

Using dynamic light scattering (DLS), a technique based on the laser diffraction technique with various scattering approaches, the mean size of the particles of silver nanoparticles (AgNPs) was ascertained. After distributing the produced sample in Milli-Q water, it was ultrasonically agitated. The solution was then filtered, and the supernatant was recovered after a 15-minute centrifugation at 25^0C and 5000 rpm. The liquid's particle distribution was examined using a computer-controlled particle size analyzer (Zetasizer Nano series Malvern Instrument Nano Zs) after diluting the supernatant 4-5 times.

FE-SEM analysis

The characteristics of the produced silver nanoparticles (AgNPs) morphology from *S. foetida* bark extract were studied by Field Emission Scanning Electron Microscope (Carl Zeiss, Germany, Merlin Compact). SEM slides were produced by spreading the solutions onto them 24 hours after $AgNO_3$ was added. The samples were coated with a tiny layer of platinum to make them conductive. After that, the samples were examined in the SEM at a 20 kV accelerating voltage.

Study of Antibacterial Activity

Agar-well diffusion method

The agar-well diffusion method has been performed using a Nutrient Agar (NA) medium. Media was prepared using distilled or deionized water and autoclaved for 15 minutes at 121°C to sanitize. pH has been maintained between 7.2 and 7.4, and it solidifies at 30-37°C in a sterilized Petri dish. Bacterial culture (*E. coli* and *S. aureus*) has been prepared by taking 4 to 5 colonies in 5 ml of 0.9% saline and adjusting to a turbidity of 0.5 Mac Farland standards. 1 ml of test strain was spread over the medium using a spreader made with a sterilized cotton swab. 4 mm diameter wells were pierced in the culture medium using a flame-tipped sterile borer, and the necessary concentrations of AgNP solution were then added to the wells. After allowing the extracts to diffuse into the media for an hour, the plates were prepared as before and incubated at 37^0C. Forty-eight hours after incubation, the plates were examined for zones of inhibition. The zone of inhibition's diameter was calculated and reported in ml. Plant extract and $AgNO_3$ solution served as the negative control. Three copies were conducted for every experiment. Three sets of experiments have also been inoculated with a control strain AMX^{30} for positive control.

RESULTS

Green synthesis of silver nanoparticles

The synthesis of *S. foetida* bark extract-loaded silver nanoparticles was conducted using three different concentrations of $AgNO_3$ solution: 0.025 M, 0.05 M, and 0.1 M. To each 80 ml of the respective aqueous $AgNO_3$ solution, 20 ml of bark extract (1.7 g/100 ml) was added at room temperature. The final mixture was stirred with a magnetic stirrer for 2.5 hours at a constant temperature between 65-70°C to achieve the desired color development and nanoparticle formation. Surface plasmon resonance is excited in an aqueous solution of silver nanoparticles, which results in their bright yellowish color. The extract's color changed from colorless to dark brown when it was combined with the Ag ion complex's aqueous solution. This resulted from the decrease in Ag+, which shows the formation of Ag nanoparticles. The synthesis and color changes of AgNPs are illustrated below in Figure 3.

Figure 3. 100 ml of synthesized nanoparticles of different concentrations.

Visual observation:

Within 15-20 minutes, there should be a noticeable color shift from transparent to yellow, signifying the creation of silver nanoparticles, as also verified by UV-visible analysis. Moreover, the color shift to a dark brown hue results from growing and concentrated silver nanoparticles. The fact that the color did not significantly alter after 30-45 minutes indicates that the reduction reaction was complete.

UV-Visible spectra analysis

The color shift indicated that when Ag ions were exposed to plant extracts, they were reduced to Ag nanoparticles. The color change is due to the Surface Plasmon Resonance phenomenon. Because the unbound electrons in the metal nanoparticles vibrate collectively in resonance with light waves, the metal nanoparticles exhibit an SPR absorption band. Around 421 nm, in the case of *S. foetida,* (Figure 4), the crisp bands of silver nanoparticles were visible. It was discovered from many publications that the AgNPs exhibit an SPR peak at about 420 nm. We discovered the SPR peak at 421 nm from our research.

Consequently, we verified that the bark extract of *S. foetida* possesses a greater capacity to convert silver ions into silver nanoparticles. This prompted us to investigate the synthesis of silver nanoparticles using bark extracts more. With a rising period, the absorption peak's strength rises. The distinctive color shift results from the SPR being excited in the metal nanoparticles shown in the insets, which show the plots of absorbance at λ_{max} (420 nm) against reaction time. After the metal ions are added to the plant extract, the reduction of the metal ions happens very quickly; within two hours, more than 90% of the reduction of Ag^{+} ions is finished. It was demonstrated that the metal particles remained stable in solution four weeks after being created. By stability, we mean that there was no noticeable change in the optical properties of the nanoparticle solutions over time. The 0.1 M $AgNO_3$ concentration proved to be the most suitable for synthesizing AgNPs in terms of yield. As the maximum absorbance is shown by 0.1 M concentration, further ATR-IR analysis, DLS analysis, Zeta-potential analysis, and SEM analysis are carried out at a concentration of 0.1 M solution.

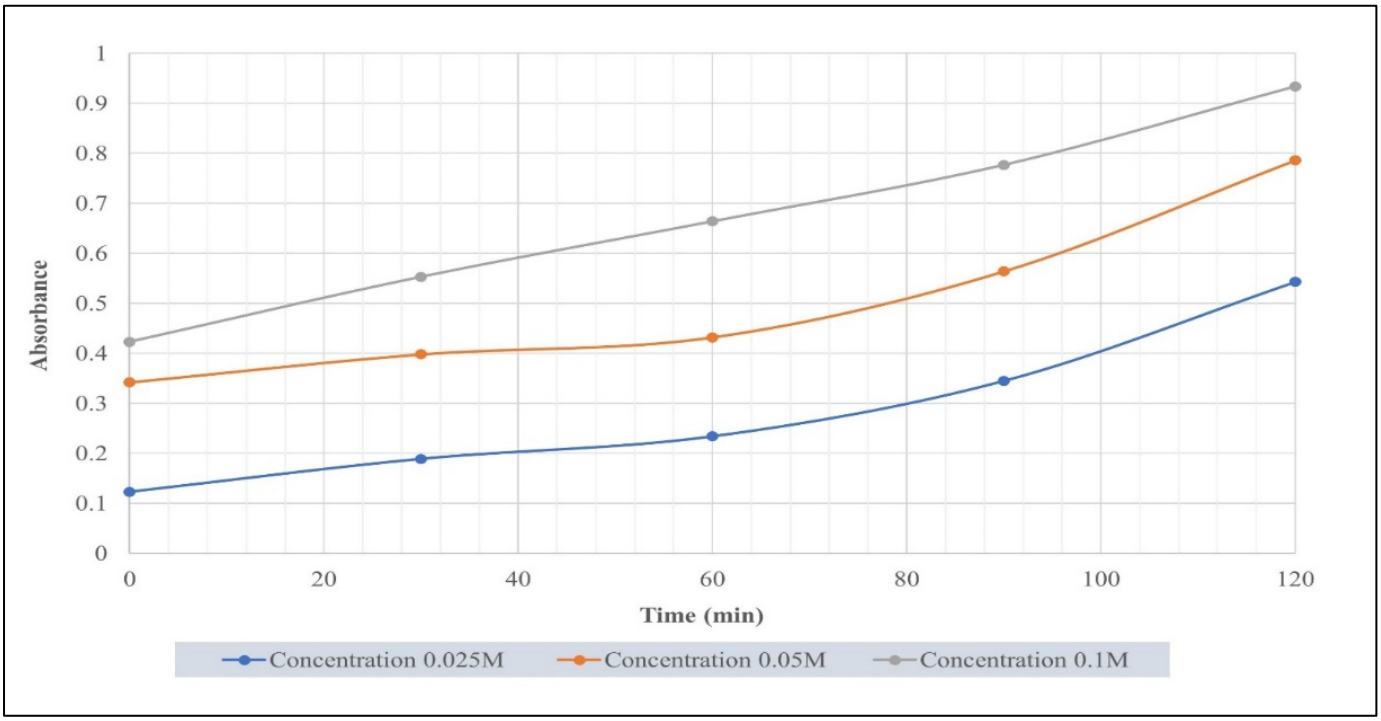

Figure 4. UV-vis spectroscopy of different concentrations of silver nanoparticles.

ATR-IR analysis

ATR-IR studies were performed to find the biomolecules needed for the capping and adequate stability of the produced metal nanoparticles. The ATR-IR spectra of silver nanoparticles (Figure 5) for the 0.1 M ratio revealed that the band between 3490 and 3500 cm^{-1} indicates phenols and O-H stretching H-bonded alcohols. The C-H bond was discovered to be stretched approximately 1500–1550 cm^{-1}, while the N–H bond was found to be stretched around 1450-1500 cm^{-1}. A peak in the IR stretched approximately 2000-2500 cm-1 is also present, indicating Silver Nanoparticles' presence. On the other hand, AgNPs were observed to extend between 500 and 550 cm^{-1}. Therefore, the synthesized nanoparticles encircled proteins and metabolites with functional groups, including terpenoids. Through the analysis of ATR-IR studies, we confirmed that proteins and amino acid residues have more vital carbonyl groups that can bind metal. This suggests that proteins may prevent agglomeration and stabilize the medium by capping Silver or other metal nanoparticles. This shows that biological molecules may have two roles in the aqueous medium: they may produce and stabilize silver nanoparticles. Carbonyl groups showed the absorption of terpenoids or flavanones on the surface of metal nanoparticles. If there is an inadequate concentration of potent ligating chemicals, terpenoids or flavanones could adsorb on metal nanoparticle surfaces through interaction through carbonyl groups or π-electrons. The reduction of the metal ions and the creation of the associated metal nanoparticles may be the result of reducing sugars in the solution. By oxidizing the aldehyde groups to carboxylic acids in the compounds, terpenoids may also reduce metal ions. These issues can be fixed once the various neem leaf extract fractions have been recognized, divided, and independently examined for the reduction of the metal ions. This study is being conducted at the moment.

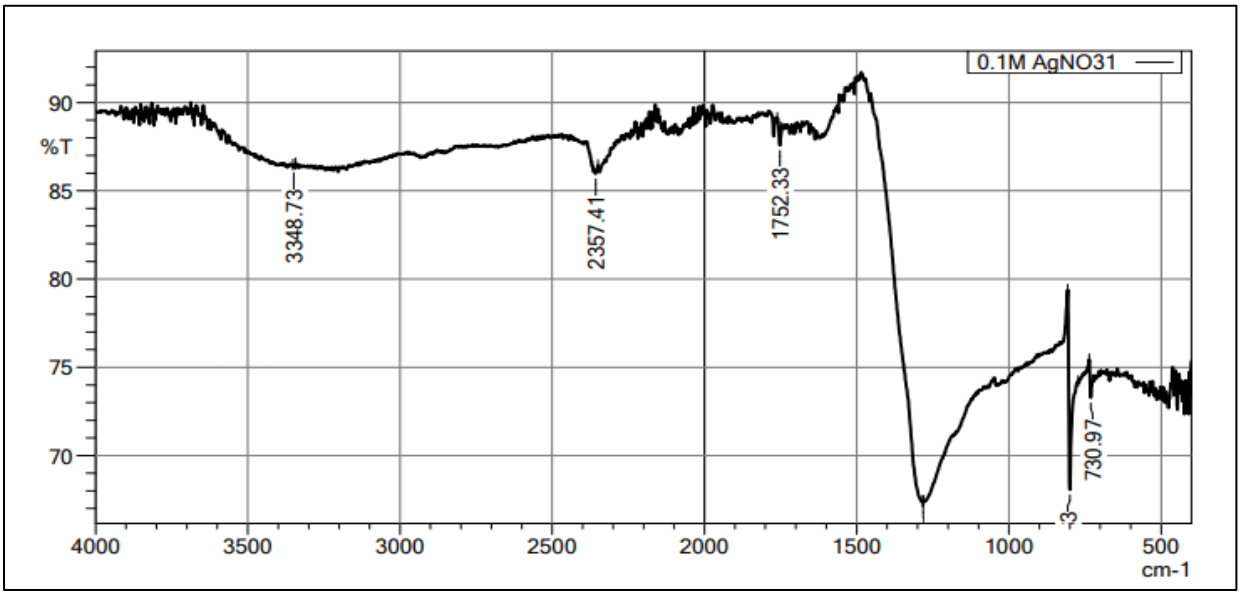

Figure 5. ATR-IR spectrum of the synthesized silver nanoparticles.

DLS analysis

The dynamic light scattering technique effectively measures particle diameters in the original grain size distribution after a reaction. Several factors, including pH value, temperature, and reaction time influence the size distribution of Ag-NPs. The pictures (Figure 6) depict the particle size distribution of AgNPs that were manufactured at 0.1 M. The colloidal solution containing silver nanoparticles (AgNPs) at a ratio of 0.1 M indicates that the particles vary in size, with some having an average size between 79 and 1209 nm.

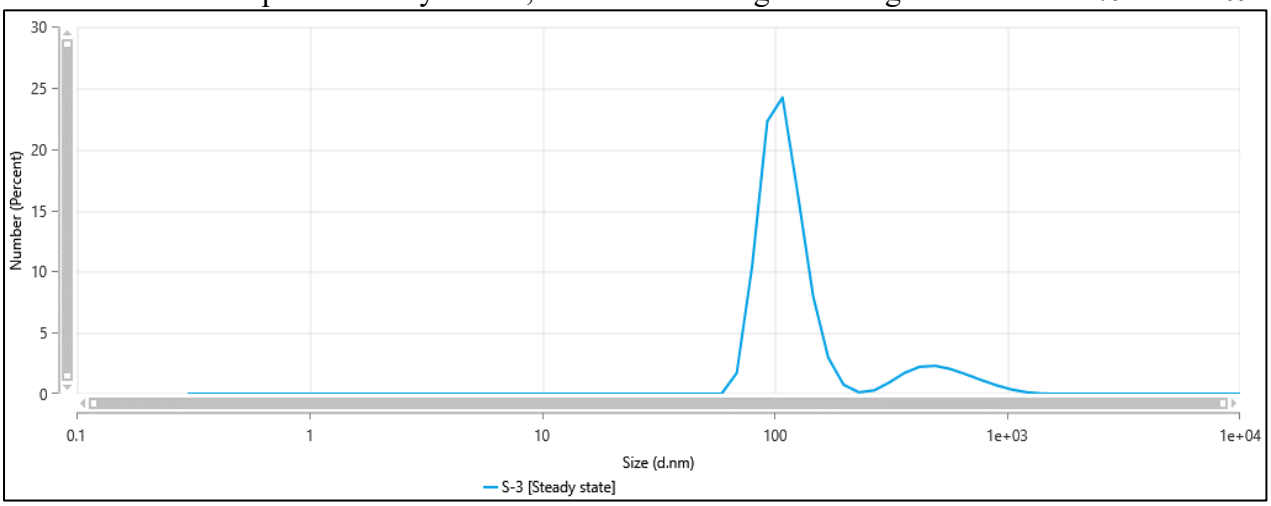

Figure 6. DLS curve of synthesized silver nanoparticles.

Zeta-Potential analysis

The Zeta potential measurements for silver nanoparticles manufactured at 0.1 M is 14.5 mV (Figure 7). Because they are so tiny, nanoparticles exhibit extreme energy instability. For the particles to stabilize themselves by agglomerate or aggregate. The nanoparticles are stable because of the potential charges on their surface. This analysis was the source of the possible charge.

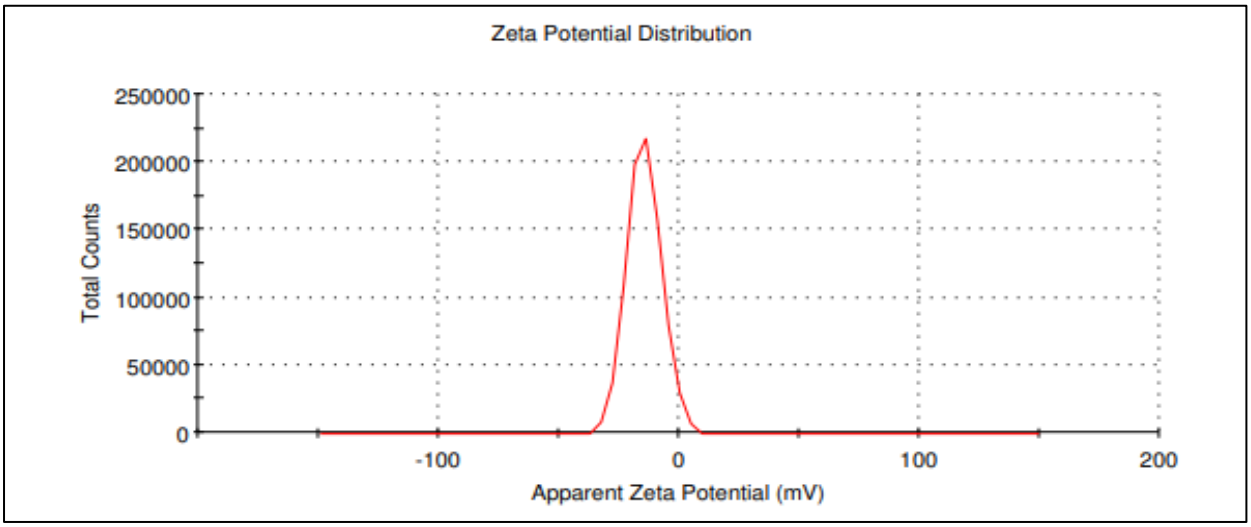

Figure 7. Zeta potential analysis for synthesized silver nanoparticles.

SEM analysis

In line with research by Ramesh *et al.,* [42] biogenically synthesized silver nanoparticles (AgNPs) were analyzed using scanning electron microscopy (SEM) to investigate their morphology and size. Further information about the size and shape

The properties of the silver nanoparticles were obtained from the SEM study. According to the experimental findings, the concentration of the produced nanoparticles in the solution affected their sizes. Specifically, at concentrations of 0.1 M, the nanoparticles exhibited sizes in the range of µm. These findings are illustrated in (Figure 8) of the study. It was observed that the size of the prepared nanoparticles exceeded the desired range of 1-100 nanometres. This size discrepancy was attributed to the presence of proteins bound to the surface of the nanoparticles. These proteins contributed to an increase in the overall size of the particles. At a concentration of 0.1 M, the particles exhibited a cuboidal shape. The change in shape was directly influenced by the concentration of the solution, as described in a study by Mohammadi *et al*.

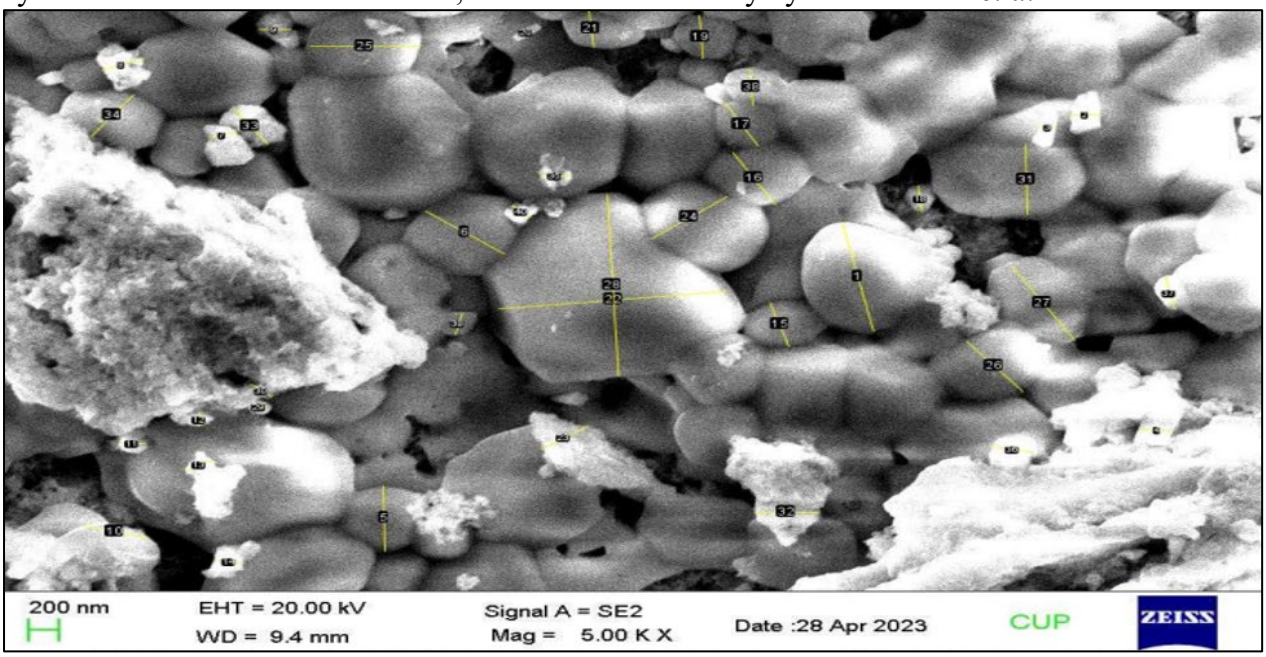

Figure 8. SEM image of synthesized silver nanoparticles.

Study of antibacterial activity

Numerous previous investigations have demonstrated the potent antibacterial properties of Ag ions and Ag-based compounds[43]. The antibacterial assay aimed to determine how sensitive standard strains were to manufactured AgNPs and plant methanolic extracts. The diameters of inhibition growth zones were measured

to evaluate the antibacterial efficacy of the extract of S. foetida, synthesized AgNPs, and antibiotics (AMX30) on microorganism strains. The *in vitro* test for antimicrobial activity revealed that AgNPs synthesis by *S. foetida* extract had an inhibitory zone and completely stopped Gram-positive and Gram-negative bacteria from growing. The antimicrobial assay showed *S.foetida* extract has antimicrobial activities against all the tested microorganisms. The bark extract's maximum activity was discovered against gram-negative bacteria *E. coli* (1.66 cm), and the highest activity of the plant-loaded AgNPs was found against gram-negative bacteria E. coli (1.74 cm), as demonstrated in Table 2 and Figure 9.

Microorganism	Sample	Concentration of drugs	Zone of inhibition	Antibacterial activity
Escherichia coli	Methanolic extract of bark	100 µg/ml	1.36 cm	Positive result
		200 µg/ml	1.45 cm	Positive result
		500 µg/ml	1.66 cm	Positive result
	Bark extract-loaded AgNPs	100 µg/ml	1.49 cm	Positive result
		200 µg/ml	1.65 cm	Positive result
		500 µg/ml	1.74 cm	Positive result
	AMX^{30} (Standard drug)	500 µg/ml	1.92 cm	Positive result
	Control (No drug-induced)	-	0 cm	Negative result
Staphylococcus aureus	Methanolic extract of bark	100 µg/ml	1.25 cm	Positive result
		200 µg/ml	1.33 cm	Positive result
		500 µg/ml	1.53 cm	Positive result
	Bark extract-loaded AgNPs	100 µg/ml	1.24 cm	Positive result
		200 µg/ml	1.45 cm	Positive result
		500 µg/ml	1.68 cm	Positive result
	AMX^{30} (Standard drug)	500 µg/ml	2.09 cm	Positive result
	Control (No drug-induced)	-	0 cm	Negative result

Table 2. Antibacterial assay and zone of inhibition.

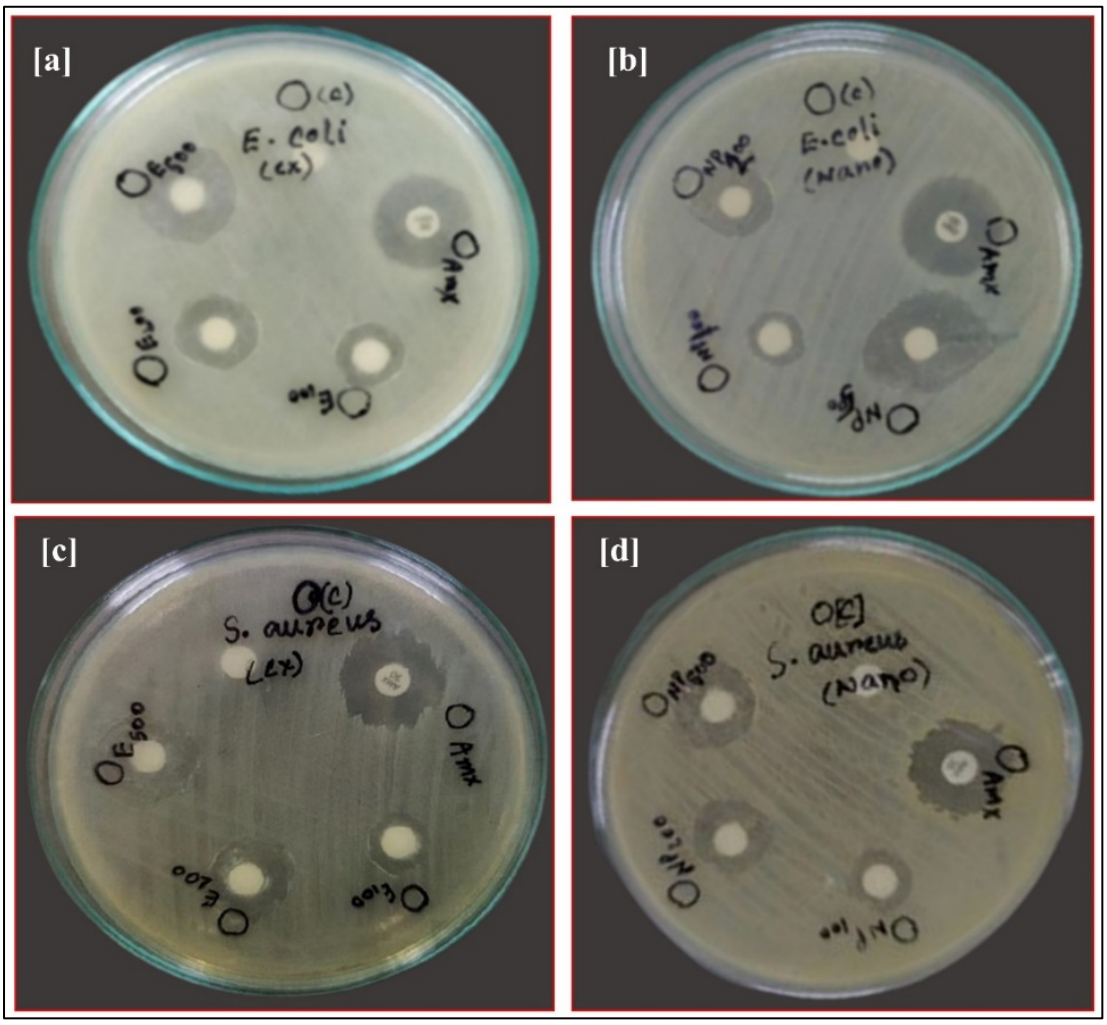

Figure 9. Antibacterial activity. [a] Zone of Inhibition against *E. coli* by different concentrations of methanolic extract. [b] Zone of Inhibition Against *E. coli* by different concentrations of AgNPs. [c] Zone of Inhibition Against *S. aureus* by different concentrations of methanolic extract. [d] Zone of Inhibition Against *S. aureus* by different concentrations of AgNPs.

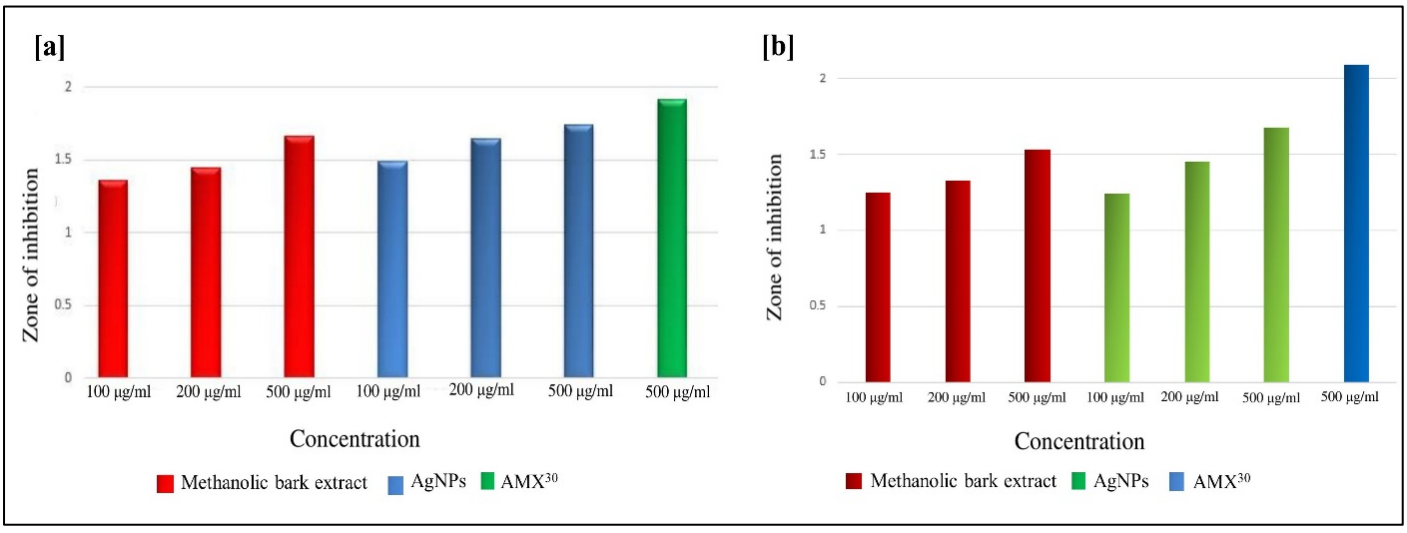

Figure 10. The antibacterial activity was quantified and represented in a bar diagram. [a] *E. coli* and [b] *S. Aureus*

DISCUSSION

Silver nanoparticles (AgNPs) are tiny particles of Silver with sizes ranging from 1 to 100 nanometers, known for their unique physical, chemical, and biological properties. Developing simple, reliable, and eco-friendly methods enhances interest in synthesizing and applying nanoparticles for the benefit of humanity. In our investigation, the bark extract and $AgNO_3$ solution were combined at room temperature, and the combination was continuously heated between 65 and 70°C for 2.5 hours while being stirred. A color shift indicates the reduction of silver ions into silver nanoparticles when exposed to plant extracts. The surface plasmon resonance phenomenon caused the silver nanoparticles to appear dark brown in an aqueous solution. The concentration and development of silver nanoparticles are indicated by the color shift from yellow to dark brown.

The presence of silver nanoparticles in the sample was confirmed by ATR-IR analysis, which showed that different phytochemicals from the bark extract were contained in the metal nanoparticles. DLS analysis revealed an average particle size of 79 nm, and SEM analysis showed the cuboidal shape of the silver nanoparticles, whereas another study by Shivakumar *et al*. by using young leaf extracts got a particle size between 30-50 nm by TEM images with less in size as compared to the average size found in this study.

This study investigated the use of silver AgNPs as an antibacterial agent, demonstrating enhanced activity against both *E. coli* and *S. aureus*. For *E. coli*, plant extract, and bark extract are loaded with AgNPs, and AMX^{30} (the standard drug) was tested with three different concentrations. At a concentration of 500 µg/ml, the bark extract loaded with AgNPs produced a maximum inhibition zone of 1.74 cm, while AMX^{30} showed a larger inhibition zone of 1.92 cm. This indicates good activity of the nanoparticles against gram-negative bacteria. For *S. aureus*, at the same concentration, the bark extract loaded with AgNPs produced an inhibition zone of 1.68 cm compared to 2.09 cm of AMX^{30}. It is primarily thought that *S. foetida* berk extract-loaded AgNPs exhibit antibacterial effects through a combination of physical interactions and chemical reactions with bacterial cells (Figure 1). The nanoparticles attach to and penetrate bacterial membranes, generate ROS, disrupt cellular structures, and interfere with metabolic processes. The bioactive compounds in the leaf extract synergistically enhance these effects, leading to potent antibacterial activity. However, no such molecular-level mechanisms were investigated in the study. The nanoparticles also showed good antibacterial activity against all concentrations tested; however, the antibacterial effect was dose-dependent. These results suggest that AgNPs are more effective against gram-negative bacteria, such as *E. coli*. AgNPs demonstrate minimal toxicity even at higher doses, making them safe and biocompatible for biomedical applications.

Additionally, the bottom-up synthesis of AgNPs is an eco-friendly and cost-effective method, ideal for large-scale production to meet industrial demands in the healthcare and environmental sectors. However, the long-term stability of these synthesized AgNPs under various storage conditions and environmental factors requires further investigation to ensure their efficacy and shelf-life. Additional research, including in vivo and clinical studies, must confirm their effectiveness and safety in real-world applications.

The green synthesis of silver nanoparticles using *S. foetida* bark extract presents a promising and eco-friendly approach in nanotechnology. This study demonstrated the effective reduction of silver ions to nanoparticles, with the bark extract acting as both a stabilizing and reducing agent. Characterization techniques such as UV-Vis spectroscopy, ATR-IR, DLS, and SEM provided valuable insights into the size, shape, and stability of the synthesized AgNPs. Moreover, the evaluation of antibacterial activity highlighted the potential of *S. foetida* bark extract-loaded silver nanoparticles as potent antimicrobial agents. These nanoparticles exhibited significant inhibition against various bacteria, underscoring their potential applications in developing new antibacterial agents for biomedical and environmental purposes. This green synthesis method offers an economical and environmentally friendly alternative to conventional chemical processes and emphasizes the importance of utilizing natural resources for nanoparticle synthesis. The eco-friendly nature of this approach aligns with the growing demand for sustainable technologies across various scientific fields. Despite the eco-friendly and sustainable approach of green synthesis of silver nanoparticles (AgNPs) using plant extracts, several disadvantages exist. The reproducibility and consistency of the nanoparticle synthesis can be

challenging due to variations in plant extract composition, which is influenced by factors like plant age, part used, and geographical location. This can lead to inconsistent particle size, shape, and distribution, affecting their stability and antibacterial efficacy.

Additionally, the scale-up for industrial production is complicated by the need for large quantities of plant material and the complexity of maintaining the biological activity of the extracts. Moreover, potential environmental and health risks arise from the disposal of large volumes of plant waste and the unknown long-term effects of biogenic AgNPs on ecosystems and human health. However, with these promising results, further research is needed to explore the full range of applications and potential toxicity of *S. foetida* bark extract-loaded silver nanoparticles. Optimizing the synthesis process for scalability and reproducibility will also be essential for practical implementation in various industries.

CONCLUSIONS

In conclusion, the synthesis, characterization, and antibacterial assessment of *S. foetida* bark extract-loaded silver nanoparticles provide valuable insights into nanotechnology. It may hold promising future possibilities across various fields. In medicine, they could revolutionize antimicrobial treatments, providing potent, broad-spectrum alternatives to traditional antibiotics, which are increasingly facing resistance. Their biocompatibility and enhanced efficacy can lead to advanced wound dressings, coatings for medical devices, and targeted drug delivery systems. In agriculture, these AgNPs can offer eco-friendly pest control and plant disease management solutions, reducing reliance on chemical pesticides. Environmental applications include water purification, where they can effectively remove contaminants and pathogens. Additionally, their integration into consumer products such as textiles, cosmetics, and packaging materials can lead to safer, more hygienic goods. This research offers a sustainable and effective solution for combating bacterial infections, paving the way for future studies and applications that bridge the gap between green synthesis and nanomaterials for improved biomedical and environmental outcomes.

FUNDING: No organization funds the work.

ACKNOWLEDGEMENT: The authors acknowledge Bharat Technology for providing the opportunity to conduct this research. Special thanks are extended to the Institute's Department of Pharmacognosy for supplying all the necessary instruments and for their cordial cooperation.

CONFLICT OF INTEREST: The authors declare no conflict of interest.

REFERENCES

1. Malik, S.; Muhammad, K.; Waheed, Y. Nanotechnology: A Revolution in Modern Industry. *Molecules* **2023**, *28* (2), 661. https://doi.org/10.3390/molecules28020661.
2. McNeil, S. E. Nanotechnology for the Biologist. *Journal of Leukocyte Biology* **2005**, *78* (3), 585–594. https://doi.org/10.1189/jlb.0205074.
3. Baig, N.; Kammakakam, I.; Falath, W. Nanomaterials: A Review of Synthesis Methods, Properties, Recent Progress, and Challenges. *Mater. Adv.* **2021**, *2* (6), 1821–1871. https://doi.org/10.1039/D0MA00807A.

4. Bharathi, D.; Diviya Josebin, M.; Vasantharaj, S.; Bhuvaneshwari, V. Biosynthesis of Silver Nanoparticles Using Stem Bark Extracts of Diospyros Montana and Their Antioxidant and Antibacterial Activities. *J Nanostruct Chem* **2018**, *8* (1), 83–92. https://doi.org/10.1007/s40097-018-0256-7.
5. Balážová, Ľ.; Čižmárová, A.; Baláž, M.; Daneu, N.; Salayová, A.; Bedlovičová, Z.; Tkáčiková, Ľ. Green Synthesis of Silver Nanoparticles and Their Antibacterial Activity. *Chem. Listy* **2022**, *116* (2), 135–140. https://doi.org/10.54779/chl20220135.
6. Khan, F.; Shahid, A.; Zhu, H.; Wang, N.; Javed, M. R.; Ahmad, N.; Xu, J.; Alam, Md. A.; Mehmood, M. A. Prospects of Algae-Based Green Synthesis of Nanoparticles for Environmental Applications. *Chemosphere* **2022**, *293*, 133571. https://doi.org/10.1016/j.chemosphere.2022.133571.
7. Nguyen, N. P. U.; Dang, N. T.; Doan, L.; Nguyen, T. T. H. Synthesis of Silver Nanoparticles: From Conventional to ‘‘odern’’Methods—A Review. *Processes* **2023**, *11* (9), 2617. https://doi.org/10.3390/pr11092617.
8. Naganthran, A.; Verasoundarapandian, G.; Khalid, F. E.; Masarudin, M. J.; Zulkharnain, A.; Nawawi, N. M.; Karim, M.; Che Abdullah, C. A.; Ahmad, S. A. Synthesis, Characterization and Biomedical Application of Silver Nanoparticles. *Materials* **2022**, *15* (2), 427. https://doi.org/10.3390/ma15020427.
9. Mikhailova, E. O. Silver Nanoparticles: Mechanism of Action and Probable Bio-Application. *JFB* **2020**, *11* (4), 84. https://doi.org/10.3390/jfb11040084.
10. Anees Ahmad, S.; Sachi Das, S.; Khatoon, A.; Tahir Ansari, M.; Afzal, Mohd.; Saquib Hasnain, M.; Kumar Nayak, A. Bactericidal Activity of Silver Nanoparticles: A Mechanistic Review. *Materials Science for Energy Technologies* **2020**, *3*, 756–769. https://doi.org/10.1016/j.mset.2020.09.002.
11. More, P. R.; Pandit, S.; Filippis, A. D.; Franci, G.; Mijakovic, I.; Galdiero, M. Silver Nanoparticles: Bactericidal and Mechanistic Approach against Drug Resistant Pathogens. *Microorganisms* **2023**, *11* (2), 369. https://doi.org/10.3390/microorganisms11020369.
12. Guo, W.; Xing, Y.; Luo, X.; Li, F.; Ren, M.; Liang, Y. Reactive Oxygen Species: A Crosslink between Plant and Human Eukaryotic Cell Systems. *IJMS* **2023**, *24* (17), 13052. https://doi.org/10.3390/ijms241713052.
13. Darojati, U. A.; Murwanti, R.; Hertiani, T. Sterqulia Quadrifida R.Br: A Comprehensive Review of Ethnobotany, Phytochemistry, Pharmacology and Toxicology. *J. Pharm. Sci. Clin. Res.* **2022**, *7* (1), 1. https://doi.org/10.20961/jpscr.v7i1.52244.
14. Mgbeahuruike, E. E.; Yrjönen, T.; Vuorela, H.; Holm, Y. Bioactive Compounds from Medicinal Plants: Focus on Piper Species. *South African Journal of Botany* **2017**, *112*, 54–69. https://doi.org/10.1016/j.sajb.2017.05.007.
15. Rahman, M. M.; Ahmad, S. H.; Lgu, K. S. *Psidium Guajava* and *Piper Betle* Leaf Extracts Prolong Vase Life of Cut Carnation (*Dianthus Caryophyllus*) Flowers. *The Scientific World Journal* **2012**, *2012*, 1–9. https://doi.org/10.1100/2012/102805.
16. Suganya, J.; Viswanathan, T.; Radha, M.; Rathisre, P. R.; Marimuthu, N. In Vitro Antibacterial Activity of Different Crude Leaves Extracts of *Sterculia Foetida* Linn. *Rese. Jour. of Pharm. and Technol.* **2017**, *10* (7), 2013. https://doi.org/10.5958/0974-360X.2017.00352.3.
17. Vital, P. G.; Jr, R. N. V.; Demigillo, J. M.; Rivera, W. L. Antimicrobial Activity, Cytotoxicity and Phytochemical Screening of Ficus Septica Burm and Sterculia Foetida L. Leaf Extracts.
18. Kavitha, M.; Vadivu, R.; Radha, R. A Review on *Sterculia Foetida* Linn. *Rese. Jour. of Pharmac. and Phytoch.* **2015**, *7* (4), 239. https://doi.org/10.5958/0975-4385.2015.00037.0.
19. Rollando, R.; Warsito, W.; Masruri, M.; Widodo, W. Potential Therapeutic Use of Sterculia Quadrifida R.Br and Sterculia Foetida Linn.: Review. *Asian J. of Plant Sciences* **2020**, *19* (4), 325–334. https://doi.org/10.3923/ajps.2020.325.334.
20. Siswadi, S.; Saragih, G. S. Phytochemical Analysis of Bioactive Compounds in Ethanolic Extract of Sterculia Quadrifida R.Br.; Malang, Indonesia, 2021; p 030098. https://doi.org/10.1063/5.0053057.
21. Xia, P.; Song, S.; Feng, Z.; Zhang, P. [Chemical constituents from leaves of Sterculia foetida]. *Zhongguo Zhong Yao Za Zhi* **2009**, *34* (20), 2604–2606.
22. Alam, N.; Banu, N.; Aziz, Md. A. I.; Barua, N.; Ruman, U.; Jahan, I.; Chy, F. J.; Denath, S.; Paul, A.; Chy, Md. N. U.; Sayeed, M. A.; Emran, T. B.; Simal-Gandara, J. Chemical Profiling, Pharmacological

Insights and In Silico Studies of Methanol Seed Extract of Sterculia Foetida. *Plants* **2021**, *10* (6), 1135. https://doi.org/10.3390/plants10061135.

23. Peláez, R.; Pariente, A.; Pérez-Sala, Á.; Larráyoz, I. M. Sterculic Acid: The Mechanisms of Action beyond Stearoyl-CoA Desaturase Inhibition and Therapeutic Opportunities in Human Diseases. *Cells* **2020**, *9* (1), 140. https://doi.org/10.3390/cells9010140.
24. Jana, K.; Ghosh, A.; Debnath, B.; Das, S. GC-MS Analysis of Phytocomponents of Methanolic Bark Extract of Sterculia Foetida. *RJPT* **2023**, 5624–5630. https://doi.org/10.52711/0974-360X.2023.00909.
25. Raveendran, P.; Fu, J.; Wallen, S. L. Completely ""reen" "Synthesis and Stabilization of Metal Nanoparticles. *J. Am. Chem. Soc.* **2003**, *125* (46), 13940–13941. https://doi.org/10.1021/ja029267j.
26. Vigneshwaran, N.; Nachane, R. P.; Balasubramanya, R. H.; Varadarajan, P. V. A Novel One-Pot ‘'reen’'Synthesis of Stable Silver Nanoparticles Using Soluble Starch. *Carbohydrate Research* **2006**, *341* (12), 2012–2018. https://doi.org/10.1016/j.carres.2006.04.042.
27. Okafor, F.; Janen, A.; Kukhtareva, T.; Edwards, V.; Curley, M. Green Synthesis of Silver Nanoparticles, Their Characterization, Application and Antibacterial Activity. *IJERPH* **2013**, *10* (10), 5221–5238. https://doi.org/10.3390/ijerph10105221.
28. Chu, W.; Wang, P.; Ma, Z.; Peng, L.; Guo, C.; Fu, Y.; Ding, L. Lupeol-Loaded Chitosan-Ag+ Nanoparticle/Sericin Hydrogel Accelerates Wound Healing and Effectively Inhibits Bacterial Infection. *International Journal of Biological Macromolecules* **2023**, *243*, 125310. https://doi.org/10.1016/j.ijbiomac.2023.125310.
29. Musa, N.; Sallau, M.; Oyewale, A.; Ali, T. Antimicrobial Activity of Lupeol and β-Amyrin Triterpenoids) Isolated from the Rhizome of Dolichos Pachyrhizus Harm. *Adv. J. Chem. A* **2023**, No. Online First. https://doi.org/10.48309/ajca.2024.387131.1380.
30. Guendouze-Bouchefa, N.; Madani, K.; Chibane, M.; Boulekbache-Makhlouf, L.; Hauchard, D.; Kiendrebeogo, M.; Stévigny, C.; Okusa, P. N.; Duez, P. Phenolic Compounds, Antioxidant and Antibacterial Activities of Three Ericaceae from Algeria. *Industrial Crops and Products* **2015**, *70*, 459–466. https://doi.org/10.1016/j.indcrop.2015.03.053.
31. Menezes-de-Oliveira, D.; Aguilar, M.-I.; King-Díaz, B.; Vieira-Filho, S. A.; Pains-Duarte, L.; Silva, G.-D. D. F.; Lotina-Hennsen, B. The Triterpenes 3β-Lup-20(29)-En-3-Ol and 3β-Lup-20(29)-En-3-Yl Acetate and the Carbohydrate 1,2,3,4,5,6-Hexa-O-Acetyl-Dulcitol as Photosynthesis Light Reactions Inhibitors. *Molecules* **2011**, *16* (12), 9939–9956. https://doi.org/10.3390/molecules16129939.
32. Ganesan, T.; Subban, M.; Christopher Leslee, D. B.; Kuppannan, S. B.; Seedevi, P. Structural Characterization of N-Hexadecanoic Acid from the Leaves of Ipomoea Eriocarpa and Its Antioxidant and Antibacterial Activities. *Biomass Conv. Bioref.* **2022**. https://doi.org/10.1007/s13399-022-03576-w.
33. Sanabria-Ríos, D. J.; Morales-Guzmán, C.; Mooney, J.; Medina, S.; Pereles-De-León, T.; Rivera-Román, A.; Ocasio-Malavé, C.; Díaz, D.; Chorna, N.; Carballeira, N. M. Antibacterial Activity of Hexadecynoic Acid Isomers toward Clinical Isolates of Multidrug-Resistant *STAPHYLOCOCCUS AUREUS* . *Lipids* **2020**, *55* (2), 101–116. https://doi.org/10.1002/lipd.12213.
34. Akbar, M.; Ali, U.; Khalil, T.; Iqbal, M. S.; Amin, A.; Naeem, R.; Nazir, A.; Waqas, H. M.; Aslam, Z.; Jafri, F. I.; Aslam, N.; Chohan, S. A. Cornus Macrophylla, the Antibacterial Activity of Organic Leaf Extracts and the Characterization of the More Lipophilic Components by GC/MS. *Molecules* **2020**, *25* (10), 2395. https://doi.org/10.3390/molecules25102395.
35. Chakraborty, B.; Kumar, R. S.; Almansour, A. I.; Perumal, K.; Nayaka, S.; Brindhadevi, K. Streptomyces Filamentosus Strain KS17 Isolated from Microbiologically Unexplored Marine Ecosystems Exhibited a Broad Spectrum of Antimicrobial Activity against Human Pathogens. *Process Biochemistry* **2022**, *117*, 42–52. https://doi.org/10.1016/j.procbio.2022.03.010.
36. Qian, W.; Yang, M.; Wang, T.; Sun, Z.; Liu, M.; Zhang, J.; Zeng, Q.; Cai, C.; Li, Y. Antibacterial Mechanism of Vanillic Acid on Physiological, Morphological, and Biofilm Properties of Carbapenem-Resistant Enterobacter Hormaechei. *Journal of Food Protection* **2020**, *83* (4), 576–583. https://doi.org/10.4315/JFP-19-469.
37. Formisano, C.; Rigano, D.; Senatore, F.; Raimondo, F. M.; Maggio, A.; Bruno, M. Essential Oil Composition and Antibacterial Activity of ***Anthemis Mixta*** and ***A. Tomentosa*** (Asteraceae). *Natural*

Product Communications **2012**, *7* (10), 1934578X1200701. https://doi.org/10.1177/1934578X1200701035.
38. Utegenova, G. A.; Pallister, K. B.; Kushnarenko, S. V.; Özek, G.; Özek, T.; Abidkulova, K. T.; Kirpotina, L. N.; Schepetkin, I. A.; Quinn, M. T.; Voyich, J. M. Chemical Composition and Antibacterial Activity of Essential Oils from Ferula L. Species against Methicillin-Resistant Staphylococcus Aureus. *Molecules* **2018**, *23* (7), 1679. https://doi.org/10.3390/molecules23071679.
39. A. Ghareeb, M.; A.H. Hamdi, S.; Fathi Fol, M.; M. Ibrahim, A. Chemical Characterization, Antibacterial, Antibiofilm, and Antioxidant Activities of the Methanolic Extract of Paratapes Undulatus Clams (Born, 1778). *J Appl Pharm Sci* **2022**. https://doi.org/10.7324/JAPS.2022.120521.
40. Zahara, K.; Bibi, Y.; Arshad, M.; Kaukab, G.; Al Ayoubi, S.; Qayyum, A. In-Vitro Examination and Isolation of Antidiarrheal Compounds Using Five Bacterial Strains from Invasive Species Bidens Bipinnata L. *Saudi Journal of Biological Sciences* **2022**, *29* (1), 472–479. https://doi.org/10.1016/j.sjbs.2021.09.006.
41. Faridha Begum, I.; Mohankumar, R.; Jeevan, M.; Ramani, K. GC–MS Analysis of Bio-Active Molecules Derived from Paracoccus Pantotrophus FMR19 and the Antimicrobial Activity Against Bacterial Pathogens and MDROs. *Indian J Microbiol* **2016**, *56* (4), 426–432. https://doi.org/10.1007/s12088-016-0609-1.
42. Rameshaiah, D. G. N.; Shabnam, S. NANO FERTILIZERS AND NANO SENSORS – AN ATTEMPT FOR DEVELOPING SMART AGRICULTURE. **2015**, *3* (1).
43. Raja, K.; Saravanakumar, A.; Vijayakumar, R. Efficient Synthesis of Silver Nanoparticles from Prosopis Juliflora Leaf Extract and Its Antimicrobial Activity Using Sewage. *Spectrochimica Acta Part A: Molecular and Biomolecular Spectroscopy* **2012**, *97*, 490–494. https://doi.org/10.1016/j.saa.2012.06.038.

Received: 1 August 2024/ **Accepted:** 3 September 2024 / **Published:** 15 September 2024

Citation: Koushik J, Somnath G, Abhijit G, Pijus P, Surashree S, Sonjit D, Biplab D. Silver Nanoparticles Loaded with Bark Extract of *Sterculia foetida*: Their Green Synthesis, Characterization, and Anti-bacterial Activity Evaluation.Bionatura Journal 2024; 1 (3) 17. ttp://dx.doi.org/10.70099/BJ/2024.01.03.17

Correspondence should be addressed to ***koushikjana880@gmail.com***

Peer review information. Bionatura thanks anonymous reviewer(s) for their contribution to the peer review of this work using https://reviewerlocator.webofscience.com/

ISSN. 3020-7886